

Brain Extraction in Multiple T1-Weighted Magnetic Resonance Imaging slices using Digital Image Processing Techniques

Kaue T. N. Duarte  Marinara A. N. Moura  Paulo S. Martins  Marco A. G. de Carvalho 

Abstract—The brain has been source of several studies in the literature, mostly due to its importance both to predict and to analyze certain diseases or conditions. Extracting the brain from patient images for medical analysis may provide useful information on prognosis. To this end, digital image processing algorithms have been applied to the medical field with a focus on the identification of the brain. This work proposes a brain extraction framework based on three major steps: 1) Data Acquisition; 2) Preprocessing; and 3) Largest Connected Component extraction. Our data are acquired following the OASIS protocol. The preprocessing step is applied in order to enhance contrast and eliminate possible noise from the T1-weighted MRI. Largest Connected Component extraction is performed by initially detecting the largest element in the image (i.e. the brain) and then by extracting it through mathematical morphology operators. The unsupervised framework extracts the brain in different axial slices without adjustments. The main contribution of this work is the automatic identification of the brain. It uses the brain in different brain slices and digital processing algorithms. Five metrics were applied to evaluate our results: Specificity, Recall, Accuracy, F-Measure, and Precision. In our first experiment, two metrics resulted in more than 90% in efficiency (Specificity and Precision), two of them surpassed 80% (F-Measure and Accuracy), and Sensitivity exceeded 70%. Our second experiment compared our work with related work in the literature, where it ranked 5th position in Sensitivity and 2nd position regarding Specificity

Index Terms—Image Processing, Skull Stripping, Brain Extraction, Image Segmentation, Medical Imaging

I. INTRODUCTION

The brain is a complex organ in a human body, containing more than 100 billion nerves with trillions of hidden connections, called synapses. More effectively, studying the brain and its functions has shown as a relevant tool to analyze certain diseases and conditions. The need for reliable tools that aims to extract the brain tissue has grown exponentially. However, the brain extraction is a challenging task, mostly due to its complexity and variation among distinct subjects.

Our goal in extracting the brain is to enable the automatic evaluation of brain processes, as well as its study, in an more efficient way, in order to support disease diagnosis, and the identification of pathologies of the human brain, e.g. Alzheimer's Disease, lesions and other diseases.

The advances in identifying brain regions using computational methods are well known in the literature since they

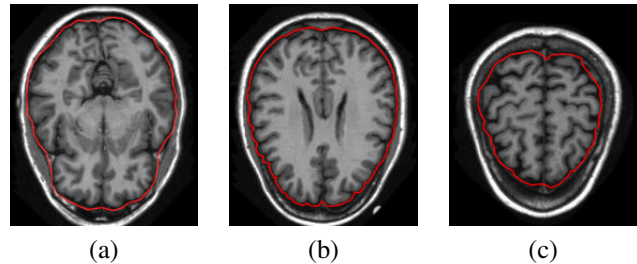


Fig. 1. Brain Extraction on: (a) slice #70, and (b) slice #100, (c) slice #130.

provide support to the radiologist analysis. This analysis is often very time-consuming when handmade, thus delaying the diagnosis and consequently the prognosis and early care.

To this date, most algorithms have focused on brain extraction and processing using software tools. In some cases, they apply Artificial Intelligence (AI) algorithms to this end. Whereas this approach may result in higher accuracy, it may imply a relatively high (and possibly prohibitive) computational cost for some applications.

In an attempt to circumvent this limitation in such cases, our work focus exclusively on digital-image processing (DIP) techniques to identify and extract the brain. We focus on extracting the brain region in multiple slices in parallel, as illustrated in Fig. 1. Notice that in the rightmost image (Fig. 1c), there are no cavities (i.e. ventricles), whereas in the central image (Fig. 1b), the two lateral ventricles are shown. This is because the lateral ventricles begin from the middle axial plane (slice #100) and continue downwards (roughly until slice #60). This is an important anatomical information for the extraction of the brain, as explained in Section III.

The main goal of this paper is to present an approach that extracts the brain (in axial projection) from the encephalon in multiple slices using DIP techniques. Our approach mainly consists in three steps: 1) Data Acquisition; 2) Preprocessing; and 3) Largest Connected Component extraction. The Data acquisition step consists in obtaining the images from OASIS dataset. The preprocessing step consists in removing the noise and enhancing the contrast of T1-weighted Magnetic Resonance Imaging (MRI) scans. The brain-extraction step uses techniques that identify the brain as a single component and extract it. The novelty in the brain extraction consists in using only DIP algorithms, thus accelerating the process.

Some contributions of this work can be highlighted: 1) this

K T N Duarte, M A N Moura, P S Martins, and M A G Carvalho work at School of Technology - University of Campinas, located in Rua Paschoal Marmo, 1888 - Jd. Nova Itália, CEP:13484-332 - Limeira, SP, Brazil.

Corresponding author: K T N Duarte, kaue.unicamp2011@gmail.com

approach works for several axial slices of the same patient, thus improving robustness; 2) the novelty in extracting the brain in several slices using exclusively DIP processes and grouping components, i.e. we do not resort to AI techniques which may be prohibitive as mentioned earlier;

This work is organized as follows: In Section II we present related work. Section III describes the workflow used to extract the brain, and the metrics to evaluate the brain. Section IV introduces our experiments, and the conclusion is presented in Section V.

II. REVIEW OF RELATED WORK

The use of Mathematical Morphology (MM) has strengthened the detection of the brain and its component in order to support the prediction of diseases. For example, Suresh [1] suggested that brain identification may be obtained by a simple thresholding followed by morphological opening to cut narrow connections. The authors used the graph cut concept to remove skull, scalp and meninx information using this concept of removing narrow connections. They first segmented the image keeping as many brain components united as possible. The remaining narrow connections were removed by Isoperimetric Graph Partitioning. Lastly, post-processing reinstates partial volumes which were wrongly removed by the cut. This approach often considers the cerebellum as part of the cerebral tissue. Their experiments showed better discrimination of brain tissue regarding Brain Extraction Tool and others.

Roslan [2] investigated the strengths and weaknesses of the Region Growing (RG) method and Mathematical Morphology applications. The flow for MM follows standard pipelines: Binarization, Morphological Segmentation, and Extraction of the Largest Connected Component. The flow of RG consists of the calculation of a seed pixel and the Region Growing between similarities of neighbors. Regarding time, MM is highly faster than RG. Additionally, RG depends on the definition of seed pixels, even they calculated automatically, once the seed pixel is wrongly defined, all the process is wasted. The accuracy is visually analyzed in the images provided: MM showed better discrimination between non-cerebral and cerebral tissues than RG.

Somasundaram [3] generated two brain extraction methods using region labeling and morphological operations. First, the image is binarized using the Ridler's method. Next, in order to isolate the scalp and brain from the background, from the skull and the CSF, the background is defined as a new label in the so-called 3-labelling process. The rough brain portion is extracted: 1) the scalp is identified due to its bright intensities; 2) the brain is generated by considering only the pixels that is not assigned to the scalp. A standard pipeline is applied by using morphological operators to remove the largest connected component. This approach reached more than 93.8% in dice similarity, sensitivity, and specificity.

Benson [4] cited the importance of working with morphological operators in different modalities (T1, T2, FLAIR). They proposed a method that could be performed in these three modalities on middle axial planes. The image is first preprocessed by adjusting the contrast using morphological

operations. Skull stripping is achieved by the Otsu thresholding and morphological operations. A binary image is generated and its largest connected component, which represents the brain tissue, is extracted. Although the authors did not present any comparison with literature methods, they stated the skull stripping process correctly distinct brain tissue from non-brain tissues.

Wiek [5] proposed a 5-step-algorithm which extracts the brain using mathematical morphology. Initially, a T1-weighted MRI slice is thresholded using an algorithm that mixes global and local information. Some morphological operators are applied to enhance the brain. In order to identify the edges highlighted in the previous step, the Canny Edge Detection algorithm was adopted. The largest connected component, which represents the brain, was then extracted. They compared with literature solution for the same problem, however, certain tools presented some limitations. The association of better results was related to their threshold as one of the basic processes.

Also, the images could be described by their histogram distributions. In Balan [6], skull stripping is addressed in 3D MRI's. The technique used consists in the analysis of unique histograms. In essence, their method attempts to partition the histogram based on the maximum deviation obtained from a Gaussian fit. First, the background is removed by analyzing the peaks of the histogram, since the background presents the same intensity values. A new histogram is generated and it is submitted to a new histogram partition analysis, thus obtaining white and gray matter. Once the thresholds are found, a rough mask is generated. The pipeline of morphological operators is applied, thus resulting in the brain. This technique reached high results considering different dataset. Using Dice Similarity, Sensitivity, and Specificity, in the first and third dataset it reached more than 98%, and in the second and the fourth one it overpassed 92%.

Subudhi [7] defined a three-step algorithm that removes the brain using Histogram Partitioning with Maximum Entropy Divergence. First, the MRI scan is enhanced by using the Particle Swarm Optimization in order to extract the blood vessels. The histogram partitioning is applied to find the gray-tone, where lies the maximum entropy divergence, giving a threshold. This threshold is used to generate a new histogram without the background information. Next, the histogram is analyzed to find a rough binary mask. At the end, a standard pipeline using morphological operations and component extraction is applied, thus yielding the brain tissue. They evaluated the proposed algorithm using specific slice of the brain in both enhanced and non-enhanced images, in terms of sensitivity, specificity, precision, and accuracy. These metrics applied to non-enhanced images reached 89.8%, 97.7%, 97.6%, and 93.7%, respectively. When applied to enhanced images, it reached 100%, 95.8%, 96.1%, and 97.9%, respectively.

Among the work that introduce Artificial Intelligence into skull stripping, Taherdangkoo [8] employed a semi-supervised Artificial Bee Colony algorithm to remove the skull. The algorithm was optimized but it kept the main idea of artificial bee colony algorithm. It was initialized defining the number of employee, onlooker and scout bees. The Cerebrospinal Fluid

(CSF) intensity in the MRI scan was defined as the food source intensity. Once the food is found, the memory of the employee bee is saved. This process is carried out using the four main orientations and the algorithm stops when all the employee bees reach the CSF intensity.

Lakshmi [9] discussed the importance in preprocessing the image before skull stripping. Their algorithm is based on two steps: 1) Preprocessing, which removes noise (using the Curvelet Transform), the artifact (often generated by hardware) and the skull (using morphological operators), and 2) Segmentation, which applied a spatial Fuzzy C-Means (clustering the similar data). They evaluated by visually comparing the skull stripping process.

Kleesiek [10] generated a 3D Deep Convolutional Neural Network to process MRI scans and perform the skull stripping. They set an CNN architecture based on seven sequential convolutional layers and one soft-max output layer. The volumes were obtained through different datasets and inserted into training set for pattern extraction processes. Their method obtained the highest average specificity measure and the highest average Dice score.

Shaswati [11] proposed the use of the rough-fuzzy connect-edless algorithm to identify the brain based on 3D volumes of T1-MR scans. The most challenging task is the definition of the membership functions for the fuzzy algorithm, and the affinity relation between them. In essence, this algorithm uses the rough set theory to identify the brain. The comparison analysis showed that the performance of this algorithm surpassed the results of well-defined skull stripping algorithms. Their algorithm performed consistently well across the datasets (simulated or real). As long as the other approaches performed better in some datasets than in others.

To supplement our related work, the following tools are used to compare our approach:

- 1) Brain Extraction Tool(BET) [12], as part of the FSL package. This model starts by generating a spherical mesh in the center of the brain, then inflated towards the border of the brain. Some advantages of BET are: its speed and being insensitive to parameters setting. However, this tool might consider false-positives and being slower when registering the brain.
- 2) The Brain Surface Extractor(BSE) [13] applies sequential steps to identify the surface: Firstly, an anisotropic diffusing filtering and edge detection is performed, followed by morphological operators to adjust the surface to the brain. One disadvantage of BSE is its dependency to parameter tuning.
- 3) 3D Skull Stripping, or 3DSkullStrip, is part of AFNI package [14], and it is considered as a modified version of BET where it applies the surface inflation procedure. One advantage is the step where it removes eyes and ventricles, in addition to other adjustments.
- 4) BridgeBurner(BB) is part of the FireVoxel tool [15], where it finds a small cubic region in the white matter, and then it computes the mean intensity in a window to create a coarse segmentation, similar as AFNI. Once detected the surface, it starts to shrink to the surface to adjust to the brain edge. One disadvantage of this

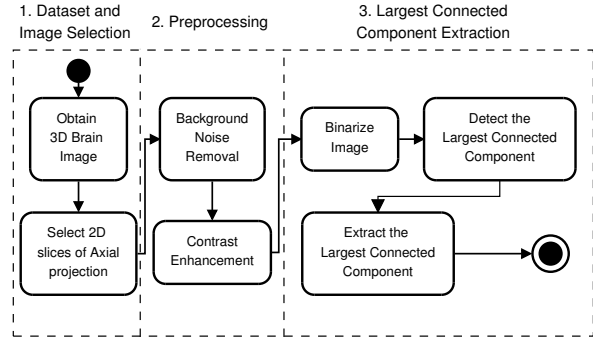


Fig. 2. Workflow of the brain extraction approach.

method is the chance to have non-brain tissue blobs in some specific parts. This algorithm often leaves the cerebrospinal fluid within the extracted brain.

- 5) GCUT is a graph cut-based approach to extract the brain [16]. Firstly, it separates the gray matter and cerebrospinal fluid by applying a threshold, which often groups the brain, skull and meninges as a single component. Graph cuts are applied to minimize the ratio between the edge cost and its volume. The last step is applied to obtain the refined brain; however, its main disadvantage is to detect the wrong edges, which may imply in an undesired brain extraction;
- 6) a preliminary step within the Freesurfer software [17], where it applies the Watershed transformer to estimate the white matter, followed by adjustments using probabilistic atlases to refine the surface and the GCUT to refine the segment.

III. PROPOSED APPROACH

This section aims to present our approach to extract the brain, which comprises the region inside the meninx. The main challenge in directly extracting the brain is the fact that it has shades of grey intensity, which differs among brain regions. This is compounded by the realization that the brain tissues, because its variation of T1-intensity according to water particles, makes it difficult to use conventional techniques such as thresholding. Therefore, the proposed workflow follows a subtraction approach, whereby unwanted objects are removed from the image step-by-step until what is left is the target object (in this case the brain). The largest component is by far the brain, so the process takes advantage of this fact by extracting the largest component. All the remaining objects, such as skull(dark intensity) and fat(bright intensity), are not considered in this work. Once this key idea is identified, the next challenge would be to figure out what are the tools and techniques that most efficiently perform each step. Fig. 2 illustrates the proposed workflow, which is detailed in the following subsections.

A. Image Acquisition

1) *Acquire 3D Brain Image*: The 3D images are obtained using the free-access OASIS dataset [18], which provides an image that is already preprocessed (image registration

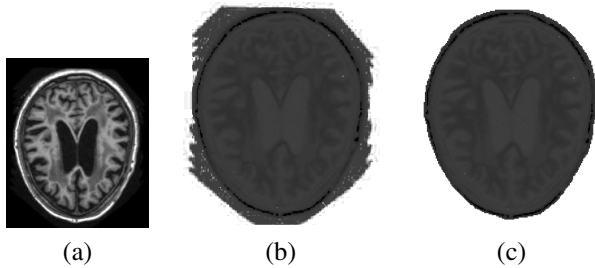


Fig. 3. Noise preview: (a) original image; (b) image enhanced for noise visualization, (c) image enhanced for noise removed visualization.

and alignment). The OASIS-1 dataset contains 3D-images composed of 208x178x178 pixels. A simple batch file was run to read all files from their repository.

2) *Extract 2D Slices of Axial projection*: In this step, we extracted only the axial (i.e. horizontal plane) projections of the brain. Out of the 178 axial slices we extracted only the 61 (from #70 up to #130) that are more related to the brain, skull, and meninx, i.e. slices below #70 do not belong to the cerebral tissue, and for the ones above #130, the cerebral tissue is scarce. These slices correspond to the images that are above the eyes and below the top.

B. Preprocessing

This section describes the steps for noise removal and contrast enhancement.

1) *Background Noise Removal*: When the slices are extracted from the volume, brighter noise appears in the background, nearby the skull region, as illustrated in Figure 3(b). The noise removal algorithm used is the one shown in Algorithm 1. The first line computes the average of the gray-tones. The second line applies a median filter using a 3x3 window. In the third line, a mask is created to remove the noise (i.e. leaving only the skull and its internal elements). The mask has zeros where the image has to be removed and ones where it should remain. In the fourth line, the mask is arithmetically multiplied by the image, thus removing the noise. Fig. 3(c) shows the image after the noise removal step.

Algorithm 1: Noise removal

```

1  $T_{image} = \text{mean}(Image);$ 
2  $imageMedian = \text{medianFilter}(image, [3, 3]);$ 
3  $mask = imageMedian > T_{image};$ 
4  $Image = mask * Image;$ 

```

2) *Contrast Enhancement*: This step is all performed using concepts and operations of mathematical morphology. The gray intensity is not normalized, i.e. it varies from image to image thus requiring the adjustment of different contrasts in different scans. Also, this steps aims to enhance the anatomical structures, since the MRI scans are in low contrast. Contrast enhancement is performed by Algorithm 2.

Once the image A is input from the previous step (Line 1), its complement B is calculated (Line 2), where L is the

Algorithm 2: Contrast enhancement

```

1  $A = \text{inputImage};$ 
2  $B = A^c = (L - 1) - A;$ 
3  $C = B \bullet SE1;$ 
4  $D = C_c = (L - 1) - C;$ 
5  $A_{diff} = A - D;$ 
6  $A_{enhanced} = A + A_{diff};$ 

```

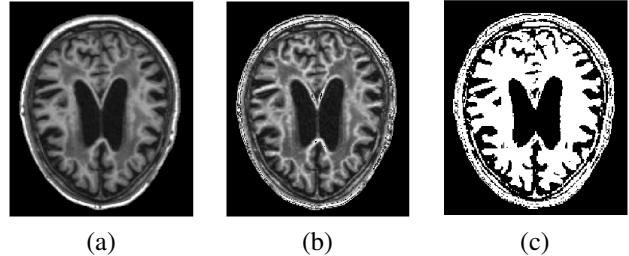


Fig. 4. Contrast enhancement: (a) original image; (b) enhanced image, (c) binarized image.

highest gray-tone available in the image A . A closing operation (Line 3) is performed using a disk structuring element $SE1$ to generate image C . After that, the complement D of image C is calculated (Line 4), using the same procedure of the second line. The difference between A and D is stored in a A_{diff} (Line 5). Finally, this difference is added to the original image A and set as the enhanced image (Line 6). In Fig. 4(b), it is illustrated the contrast enhancement based on the algorithm proposed by Benson [4].

C. Largest Connected Component Extraction

This step consists of image binarization, and detection and extraction of the largest connected component. We explain each one as follows.

1) *Image Binarization*: Image binarization (Fig. 4) is carried out with the Otsu threshold algorithm, in order to facilitate the detection of the brain components using morphological operators.

2) *Detection of the Largest Connected Component*: The brain is the largest connected component (LCC) in the middle axial slices of a MRI scan. For these scans, the work of Benson *et. al.* is known to be an adequate approach for brain extraction. Their image set may be considered a near best-case scenario, i.e. one single slice in the middle scan. We remove this restriction by allowing several slices from multiple axial areas, including the top ones (near worst-case scenario). However, three limitations can be identified: 1) *Connected skull and brain*: if brain and the skull emerge as single connected component after the labeling of the binarization process, their algorithm does not work. In Fig. 6(a) both brain and skull have the same color, i.e. they are not separated; 2) *Disconnected Brain*: The brain does appear as a single connected component, as can be seen in Fig. 6(b), i.e. the green area in the middle indicates it is not a single component as desired. 3) *Single-middle axial slice*: it was applied to a single slice and it is quite specific for the middle axial

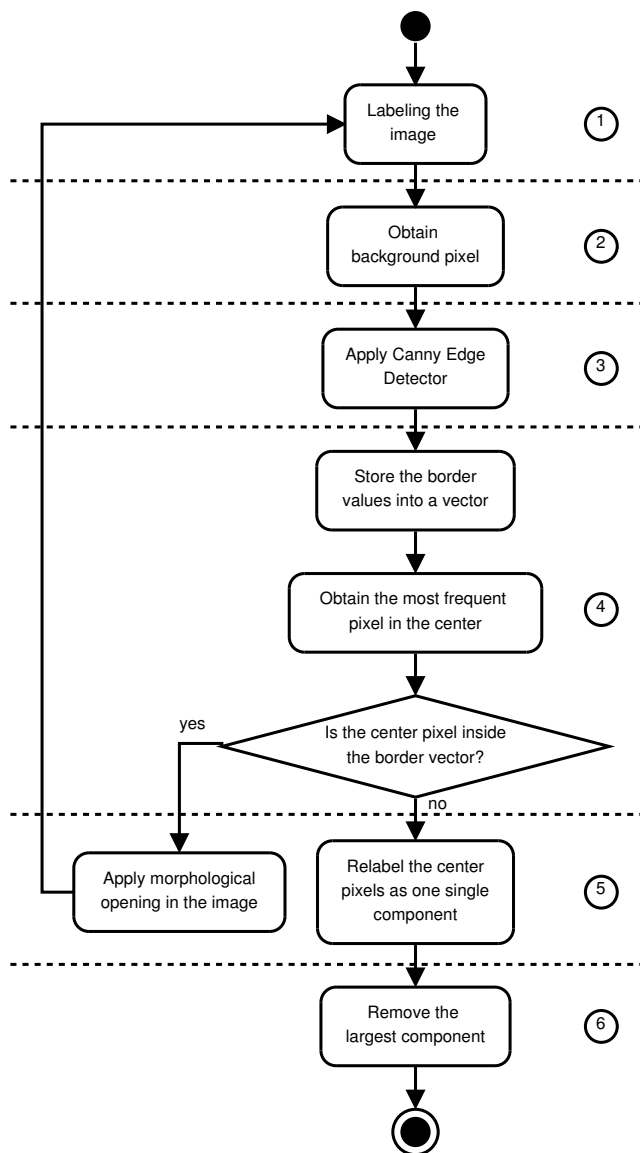


Fig. 5. Workflow for brain extraction block.

slices, i.e. closer to the top, the skull becomes the LCC, thus requiring an adaptation; Furthermore, some generalization is desired in our approach since we are dealing with a relatively larger number of slices (i.e. 61) that present brain variations in size or structure and possible abnormalities (e.g. due to either equipment defects or disease). Note: If a work is dealing with one single slice, or even with neighbor slices, this steps could be reduced or even removed.

The first sub-step defines the number of connected components and where they are located. The assumption is that, apart from the background, the brain is the largest connected component in the middle axial slices. The workflow (Fig. 5) addresses these three issues.

- 1) *External skull-border identification*: First, to find out whether the brain and the skull are a single component, we applied the following procedure: The border of the component is identified by using the Canny edge detector. The labels of the border (i.e. the skull) are

computed and then stored in a vector;

- 2) *Removal of the lateral ventricles*. The second step is to store the most frequent label in the background (i.e. avoiding remaining noise).
- 3) Thirdly, this step is responsible for computing the label that most occurs in the center that is different of most frequent label in the background, using a 25x25 window positioned in the center of the image, and store this into a vector that corresponds to the center. If this vector is inside the vector of the labels, it means that the brain is connected to the skull. So, we applied an opening operation using a disk as structural element. This validation is recursively applied until the brain separates itself from the skull. Of course, the kernel of the structural element increases at each iteration. This way we can overcome the first challenge and separates the brain from the skull. Fig. 6 illustrates the Largest Component detection.

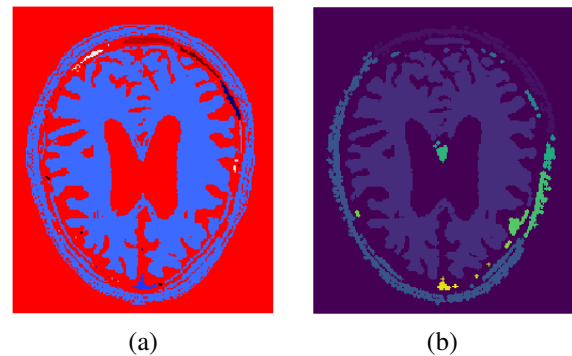


Fig. 6. Largest component detection (images were recolored using pseudo-colours for visualization purposes): (a) first process did not recognize the brain and the skull separately; (b) image after the opening operator application, separating brain from skull.

However, the brain may not be all connected, so we relabel some connected components. We have a hypothesis that the center of the image always corresponds to the brain, then, any label in the center of the image must have the same value. The same *valCenter* is used to relabel the image, every label inside the 25x25 window in the center is labelled as the label that most occurs in the center, except the background. For further information, this step is illustrated in Fig. 7(a). Using this, we overcame the second challenge.

- 3) *Extract the Largest Connected Component*: In order to extract the largest connected component, we connected the border in order to form an convex object. Using this, we avoid to lose too much information of those parts in the external brain that was not connected in the step of connection. Fig. 7 illustrates this step.

D. Implementation

Our approach was entirely implemented using the following freely-available packages:

- 1) We used the Matlab r2018a to slice the volumes as input in our approach;

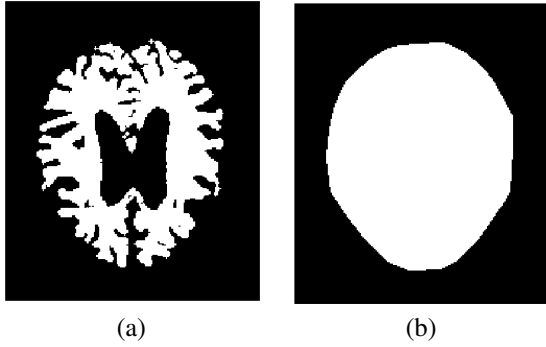


Fig. 7. Steps from grouping into a single component and convex object generation: (a) after the grouping component step; (b) convex forming application.

- 2) Our preprocessing step used Python 2.7 Jupyter Notebook. To avoid recoding, additional packages were included, such as: Scikit-image, and Scipy;
- 3) The brain extraction was performed using Python 2.7;
- 4) The evaluation was performed both in Python 2.7 and Matlab r2018a.

More information about our approach, including the OASIS identification per subject, preprocessing and brain extraction codes, slicing program, and result evaluation are available on our GitHub repository [19].

E. Metrics

To evaluate this work, we adopted the following metrics: 1) Precision (P); 2) Recall (R), also known as Sensitivity; 3) F-measure (F); 4) Specificity (S); 5) Accuracy (A).

These metrics are calculated based on the operators false-positive(FP), false-negative(FN), true-positive(TP), true-negative(TN). They are obtained using:

$$R = \frac{TP}{TP + FN}, \quad S = \frac{TN}{FP + TN}, \quad (1)$$

$$P = \frac{TP}{TP + FP}, \quad F = 2 \times \frac{P * R}{P + R}, \quad (2)$$

$$A = \frac{TP + TN}{TP + TN + FP + FN}. \quad (3)$$

Note that in brain extraction, a TP corresponds to a pixel where it is labeled as representing the brain by both our approach and the ground-truth; FN indicates the case where the approach finds a non-brain (*i.e.* background) pixel whereas the ground-truth found a brain pixel; A FP occurs when our approach identifies a brain pixel, but it is in fact a non-brain pixel set by the ground-truth. A TN is obtained whenever a pixel is labeled as non-brain area by both our approach and the ground-truth.

IV. CASE STUDY AND RESULTS

In this section we present our case studies to evaluate, using several metrics, the approach for brain extraction.

A. First Case: Comparing our Brain Extraction Approach with the Ground-Truth

In our first case, we calculated the efficiency of our approach according to five evaluation metrics. We defined 61 axial slices for each 3D projection (from slice # 70 to # 130). We used all the OASIS-1 dataset, *i.e.* 430 samples. The threshold chosen was provided by the OASIS-1 dataset (#100). Fig. 8 shows the efficiency of the brain extraction process regarding Recall, Precision, F-Measure, Accuracy, and Specificity. We reach this efficiency by comparing the resulting image with the images that were provided from the dataset. Fig. 9 illustrates the correlation among the efficiency metrics.

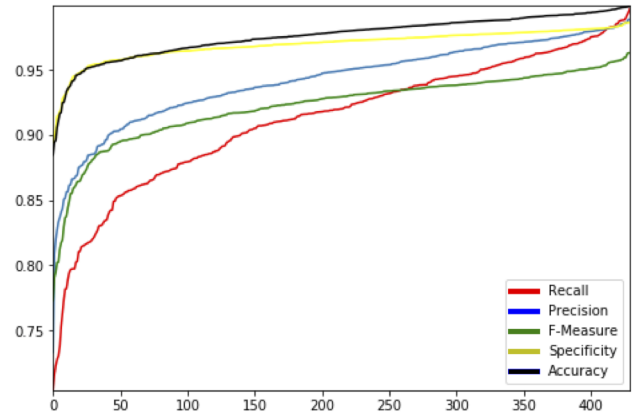


Fig. 8. Brain-extraction efficiency per number of patients.

We first calculated the efficiency for each slice. Next, an average efficiency from all slices was performed for each patient. Finally, the overall efficiency was calculated for each metric and using all the patients.

Specificity and Accuracy were the best evaluation metric (> 90%), whereas Recall was (> 70%). However, it is import to emphasize that the proposed algorithm is capable of segmenting brain images regardless of their position in the encephalon (Table I).

B. Second Case: Comparing our Approach with Relevant Related Work

As our second experiment, our approach is compared with relevant work in the literature. Table II presents the comparison

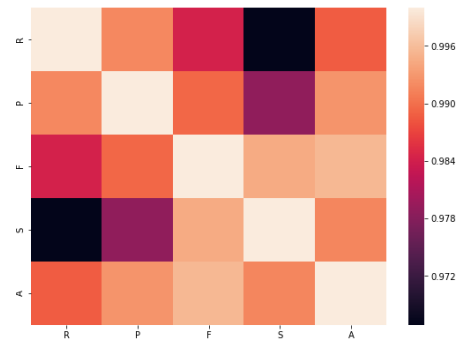


Fig. 9. Pearson's correlation between the metrics.

TABLE I

SUMMARY OF THE EVALUATION OF BRAIN EXTRACTION GROUPED BY EFFICIENCY RANGES

Range	Recall	Precision	F-Measure	Specificity	Accuracy
[0.7,0.8]	17	1	3	0	0
(0.8,0.9]	123	41	64	2	3
(0.9,1.0]	290	388	363	428	427

TABLE II

COMPARISON WITH THE LITERATURE ACCORDING TO SPECIFICITY AND SENSITIVITY METRICS

Method	Sensitivity(%)	Specificity(%)
BET [12]	92.5	94.2
BSE [13]	97.1	64.9
3dSkullStrip [14]	90.6	96.2
BB [15]	80.6	98.8
GCUT [16]	95.2	92.9
Freesurfer [17]	94.8	94.0
Our approach	91.2	96.9

between our work and the literature. To avoid any bias regarding dataset and imaging type, we followed certain criteria: 1) the method needs to use OASIS dataset as input; 2) only T1-weighted MR scans are considered; 3) same evaluation metrics to compare.

Our approach ranked the 5th position regarding Sensitivity, and it reached the 2nd position regarding Specificity. Fig. 10 illustrates the comparison according to the evaluation metrics.

V. SUMMARY AND CONCLUSION

There is currently available a significant number of open-access medical image repositories, some of them may be quite complex and multi-modal. With the improvement of data acquisition and data mining techniques, these databases may grow exponentially. However, if this growth is not paralleled with the development of efficient DIP methods and the support of automation tools that are capable of exploring these large databases within feasible time, one may not take full advantage of this wealth of information. A bottleneck is formed where these images accumulate without being able to be explored

by the medical community in their pursuit of the cure of many diseases. Clearly, faster and more efficient algorithms are desired that are capable of extracting and processing information from these databases.

One advantage of this work is the increasing in research to extract the brain to serve as a marker for diseases. Thus, it may be beneficial to digitally extract the brain from images of the encephalon to allow an easier and detailed examination (prognosis). In this work, we proposed an unsupervised framework to extract the brain from axial slices of the brain in T1-weighted MR images using digital-image processing techniques. In essence, according to the proposed approach, the brain was extracted by first applying some preprocessing and then extracting the brain. Preprocessing adjusts the images by removing background noise and enhancing contrast.

This framework employed DIP approaches in every step performed. One limitation is that the MRI should be registered and centralized in order to insert them in the process. However, for datasets that are not registered/centralized, this can be accomplished by adding a simple procedure that locates the largest and smallest radius of the slice.

The proposed framework was adjusted for T1-Weighted MR images; T2-Weighted, Proton-Density images or another type of modality may not yield good results, thus requiring additional adjustments in coding. The advantage of this work are the use of one unsupervised process to interpret and segment different slices and patients without changing the coding. Additionally, this process may be applied to a single slice, not requesting the entire volume to extract the brain (*i.e.* saving computational effort).

Our results were assessed based on quantitative metrics (Specificity, Recall, F-measure, Precision, and Accuracy). Two experiments were performed: Our first experiment was regarding the five metrics. Specificity and Precision were superior to 90%, F-Measure and Accuracy surpassed 80%, and Recall was better than 70%. In the second experiment, which analyzed other work in the literature, our approach ranked the 5th position regarding Sensitivity, and it ranked the 2nd considering Specificity.

The purpose of this research was to provide a support to medical examination. The process was performed for entire dataset without changing parameters using the OASIS-1 dataset. Future work should consider other planes such as the sagittal (*i.e.* longitudinal plane) and the coronal (*i.e.* frontal plane), which would require a different procedure and approach.

ACKNOWLEDGEMENT

The authors thank FAPESP and CAPES(Brazil) for financial support. Data were provided by OASIS: Cross-Sectional: Principal Investigators: D. Marcus, R. Buckner, J. Csernansky J. Morris; P50 AG05681, P01 AG03991, P01 AG026276, R01 AG021910, P20 MH071616, U24 RR021382.

REFERENCES

- [1] S. A. Sadananthan, W. Zheng, M. W. Chee, and V. Zagorodnov, "Skull stripping using graph cuts," *NeuroImage*, vol. 49, no. 1, pp. 225 – 239, 2010.

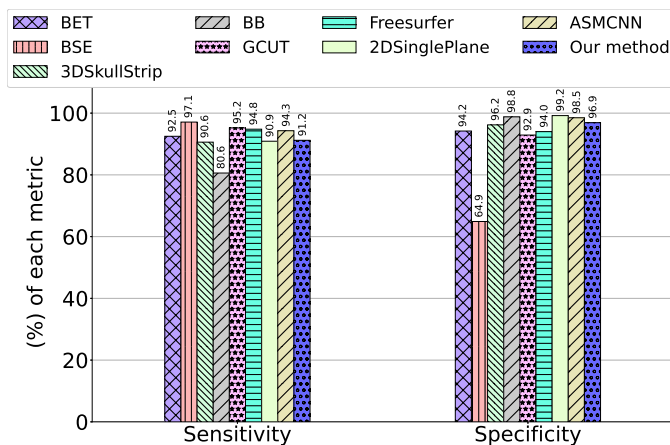


Fig. 10. Comparison with related work

- [2] R. Roslan, N. Jamil, and R. Mahmud, "Skull stripping magnetic resonance images brain images : Region growing versus mathematical morphology," 2011.
- [3] K. Somasundaram and T. Kalaiselvi, "Automatic brain extraction methods for t1 magnetic resonance images using region labeling and morphological operations," *Computers in Biology and Medicine*, vol. 41, no. 8, pp. 716 – 725, 2011.
- [4] B. C. C. and L. V. L., "Morphology based enhancement and skull stripping of mri brain images," in *2014 International Conference on Intelligent Computing Applications*, pp. 254–257, March 2014.
- [5] J. Świebicka Wiek, "Skull stripping for mri images using morphological operators," vol. 9842, pp. 172–182, 09 2016.
- [6] A. G. Balan, A. J. Traina, M. X. Ribeiro, P. M. Marques, and C. T. Jr., "Smart histogram analysis applied to the skull-stripping problem in t1-weighted mri," *Computers in Biology and Medicine*, vol. 42, no. 5, pp. 509 – 522, 2012.
- [7] A. Subudhi, J. Jena, and S. Sabut, "Extraction of brain from mri images by skull stripping using histogram partitioning with maximum entropy divergence," in *2016 International Conference on Communication and Signal Processing (ICCSP)*, pp. 0931–0935, April 2016.
- [8] T. Mohammad, "Skull removal in mr images using a modified artificial bee colony optimization algorithm," *Technology and Health Care*, vol. 22, no. 5, p. 775–784, 2014.
- [9] A. Lakshmi, T. Arivoli, and R. Vinupriyadharshini, "Noise and skull removal of brain magnetic resonance image using curvelet transform and mathematical morphology," in *2014 International Conference on Electronics and Communication Systems (ICECS)*, pp. 1–4, Feb 2014.
- [10] J. Kleesiek, G. Urban, A. Hubert, D. Schwarz, K. Maier-Hein, M. Bendszus, and A. Biller, "Deep mri brain extraction: A 3d convolutional neural network for skull stripping," *NeuroImage*, vol. 129, pp. 460 – 469, 2016.
- [11] S. Roy and P. Maji, "An accurate and robust skull stripping method for 3-d magnetic resonance brain images," *Magnetic Resonance Imaging*, vol. 54, pp. 46 – 57, 2018.
- [12] S. M. Smith, "Fast robust automated brain extraction," *Human Brain Mapping*, vol. 17, pp. 143–155, Nov. 2002.
- [13] D. W. Shattuck, S. R. Sandor-Leahy, K. A. Schaper, D. A. Rottenberg, and R. M. Leahy, "Magnetic resonance image tissue classification using a partial volume model," *NeuroImage*, vol. 13, pp. 856–876, May 2001.
- [14] "Analysis of functional neuroimages." <http://afni.nimh.nih.gov>.
- [15] A. Mikheev, G. Nevsky, S. Govindan, R. Grossman, and H. Rusinek, "Fully automatic segmentation of the brain from t1-weighted MRI using bridge burner algorithm," *Journal of Magnetic Resonance Imaging*, vol. 27, pp. 1235–1241, May 2008.
- [16] S. A. Sadanathan, W. Zheng, M. W. Chee, and V. Zagorodnov, "Skull stripping using graph cuts," *NeuroImage*, vol. 49, pp. 225–239, Jan. 2010.
- [17] F. Ségonne, A. Dale, E. Busa, M. Glessner, D. Salat, H. Hahn, and B. Fischl, "A hybrid approach to the skull stripping problem in mri," *NeuroImage*, vol. 22, no. 3, pp. 1060 – 1075, 2004.
- [18] D. S. Marcus, T. H. Wang, J. Parker, J. G. Csernansky, J. C. Morris, and R. L. Buckner, "Open access series of imaging studies (OASIS): Cross-sectional MRI data in young, middle aged, nondemented, and demented older adults," *Journal of Cognitive Neuroscience*, vol. 19, pp. 1498–1507, Sept. 2007.
- [19] https://github.com/KaueTND/Brain_Extraction_T1wMRI



Kauê Tartarotti Nepomuceno Duarte received a B.Sc. degree in System Analysis at University of Campinas (São Paulo, Brazil), a M.Sc. in texture contributions to image processing at the same university (2017), and a Ph.D. in Alzheimer's Disease prognosis by means of Image Retrieval and Machine Learning (2021), with a sandwich internship at University of Calgary (Canada) between 2019 and 2020. His main research interest are machine learning and image processing in the medical field. He is currently the Stroke prediction using Autoencoders

as a Postdoctoral Fellow at University of Calgary (Canada).



Marinara Andrade do Nascimento Moura received her degree in Science and Technology and Civil Engineering at the Federal University of the Semi-Arid Region (UFERSA), with a one-year and a half scholarship at the University of Wisconsin. She holds a Master's Degree at the University of Campinas (UNICAMP), funded by FAPESP (Brazil), in the Material Sciences field. She is currently a Ph.D. candidate at the same university in the Civil Construction area. Her main interests include inspections, structures diagnosis, technological control of materials, and non-destructive tests with ultrasound.



Marco Antonio Garcia de Carvalho received a B.Sc. degree in Electrical Engineering at the Universidade Federal do Rio Grande do Norte (Natal, Brazil, 1994), a M.Sc. degree in image processing at the School of Electrical and Computer Engineering (University of Campinas, Brazil, 1997) and a Ph.D. degree in image processing at School of Electrical and Computer Engineering (University of Campinas, Brazil, 2004). He held a sandwich stage position from 2001 to 2002 at the École Sup. d'Ingenieurs en Electrotechnique et Electronique - ESIEE (France).

His main research interests are in the areas of image processing and analysis, computer vision and the use of ICT resources in teaching and learning. He is currently professor at the School of Technology - University of Campinas



Paulo Sergio Martins Pedro received a Ph.D. in Computer Science at the University of York (England) in 2000. Dr. Paulo Martins got his master's degree in Mechanical Engineering from the Federal University of Santa Catarina (1993). He is currently a professor at UNICAMP, giving classes and supervising in Systems Analysis and Information Systems.

ACRONYMS

3dSkullStrip	3D Skull Stripping
BB	BridgeBurner
BET	Brain Extraction Tool
BSE	Brain Surface Extractor
GCUT	Graph cut-based